Published in final edited form as:

Magn Reson Med. 2021 January ; 85(1): 42–48. doi:10.1002/mrm.28405.

Trehalose as an alternative to glycerol as a glassing agent for in vivo DNP MRI

Jeffrey R. Brender[1], **Shun Kishimoto**[1], **Gareth R. Eaton**[2], **Sandra S. Eaton**[2], **Yu Saida**[1], **James Mitchell**[1], **Murali C. Krishna**[1]

[1]Radiation Biology Branch, Center for Cancer Research, National Cancer Institute, National Institutes of Health, Bethesda, MD, USA

[2]Department of Chemistry & Biochemistry, University of Denver, Denver, CO, USA

Abstract

Purpose: In dynamic nuclear polarization (DNP), the solution needs to form a glass to attain significant levels of polarization in reasonable time periods. Molecules that do not form glasses by themselves are often mixed with glass forming excipients. Although glassing agents are often essential in DNP studies, they have the potential to perturb the metabolic measurements that are being studied. Glycerol, the glassing agent of choice for in vivo DNP studies, is effective in reducing ice crystal formation during freezing, but is rapidly metabolized, potentially altering the redox and adenosine triphosphate balance of the system.

Methods: DNP buildup curves of ^{13}C urea and alanine with OX063 in the presence of trehalose, glycerol, and other polyol excipients were measured as a function of concentration. T_1 and T_m relaxation times for OX063 in the presence of trehalose were measured by EPR.

Results: Approximately 15–20 wt% trehalose gives a glass that polarizes samples more rapidly than the commonly used 60%-wt formulation of glycerol and yields similar polarization levels within clinically relevant timeframes.

Conclusions: Trehalose may be an attractive biologically inert alternative to glycerol for situations where there may be concerns about glycerol's glucogenic potential and possible alteration of the adenosine triphosphate/adenosine diphosphate and redox balance.

Keywords

dynamic nuclear polarization; glassing; OX063; EPR; relaxation

1 | INTRODUCTION

Dissolution dynamic nuclear polarization (DNP) has opened a unique window into cellular metabolism by allowing the noninvasive tracking of exogenous metabolic tracers.[1,2]

Correspondence: Murali K. Cherukuri, Biophysics Section, Radiation Biology Branch, Center for Cancer Research, National Cancer Institute, Building 10, Room B3 B35, NIH, Bethesda, MD 20892-1002, USA., murali@helix.nih.gov.

CONFLICT OF INTEREST

The authors declare that they have no conflicts of interest.

By probing the activity of specific targeted enzymes rather than measuring absolute concentrations of metabolites, dissolution DNP has an advantage in isolating specific metabolic activities over static techniques such as magnetic resonance spectroscopic imaging (MRSI), which measure an equilibrium state that may stem from many processes. However, the widespread use of dissolution DNP is limited by the availability of suitable metabolic tracers. Most dissolution DNP studies to date have used pyruvic acid as a tracer. Pyruvate's dominance in DNP research is partly because of the central position pyruvate occupies in glucose metabolism,[3] but also because of its physical properties. In contrast to most other metabolites, pyruvic acid is a liquid at room temperature. The liquid state of pyruvic acid ensures the radical is evenly mixed throughout the sample. In a solid sample dissolved in water, phase separation can occur during freezing. This is problematic as transfer efficiency from the radical to the nuclei of interest in DNP is steeply nonlinear with respect to the radical-nuclear spin distance.[4,5] Clustering of the radical species caused by phase separation increases the median radical-nuclear spin distance and may result in sharply reduced transfer efficiencies and poor signal in DNP.

To reduce phase separation during freezing, glassing agents are commonly employed in studies of non-self–glassing tracers.[6] Glycerol has emerged as the glassing agent of choice for in vivo studies[7] based on its favorable safety profile[8] and relatively high glassing efficiency. Although glycerol is safe at the concentrations used in DNP studies,[8] it is not metabolically inert.[9] Glycerol is rapidly transported into the cell by aquaporin[10] and is readily metabolized to glyceraldehyde-3-phosphate, consuming adenosine triphosphate (ATP) and flavin adenine dinucleotide (FAD) in the process. It may, therefore, potentially perturb measurements of the citric acid cycle by the consumption of ATP during the phosphorylation to glycerol-3-phosphate and by alteration of the $FAD/FADH_2$ and NAD (nicotinamide adenine dinucleotide)/NADH cytosolic redox balance from the glycerol-3-phosphate shuttle.

An improved glassing agent with a favorable safety profile that does not affect metabolism would help expand the clinical translation of DNP beyond pyruvate to other metabolic tracers. Trehalose is a nonreducing disaccharide commonly used as a pharmaceutical excipient to stabilize proteins in an immobile glass matrix.[11] Trehalose has an unusually high glass transition temperature on account of its anisotropic hydrogen bonding pattern,[12] which inhibits ice nucleation[12] and favors the formation of amorphous glasses over ordered crystalline solids or liquids. Clinical tests of trehalose intravenous (IV) injections have not shown side effects with concentrations as high as 9% wt%, far exceeding the 0.5–1% range expected in dissolution DNP after the filtration step. In contrast to glycerol, trehalose is only metabolized in the small intestine where trehalase is present and is, therefore, metabolically inert in IV injections (<0.5% is absorbed by passive diffusion in humans).[13] We show here that glasses containing ~15% trehalose give equilibrium polarizations similar to the commonly used glycerol formulation, but at much faster polarization rates.

2 | METHODS

2.1 | Dynamic nuclear polarization

We hyperpolarized 4.5M [1-^{13}C]urea or 3M [1-^{13}C]glycine (30 μL), containing 15mM OX063, and the indicated amounts of glassing agents, at 3.35 T and 1.4 K using the Hypersense DNP polarizer (Oxford Instruments, Abingdon, UK) according to the manufacturer's instructions using a microwave frequency of 94.116 GHz. Polarization buildup rates were calculated assuming single exponential growth. For the mouse imaging experiment, 100 μL of hyperpolarized urea was rapidly dissolved in 4.5 mL of HEPES-based buffer before being intravenously injected through a catheter placed in the tail vein of the mouse (12 μL/g body weight). Spectra were recorded on a 3T MR Solutions (Guildford, UK) scanner.

2.2 | EPR studies

Electron spin relaxation times of 15mM OX063 trityl samples in water:trehalose solutions were measured at 5K using a Bruker E580 pulsed EPR spectrometer (Bruker, Kontich, Belgium) with the sample cooled in a He gas atmosphere using an Oxford CF935 cryostat and a Bruker/ColdEdge "Stinger" closed-cycle He cooling system. With trehalose present, T_m and T_1 were measured by spin-echo methods.[14] T_1 values were calculated from UPEN analysis[15,16] of inversion recovery experiments using 100 exponentials without variable smoothing and an additional nonnegativity constraint with most measurements made near the peak of the field-dependent spectrum. The signal detection gate encompassed about half of the width of the echo and free induction decay (FID) measurements integrated most of the FID intensity. Without trehalose, the EPR signal exhibited an FID that could not be suppressed with attempts to decrease the magnetic field homogeneity, so an echo could not be observed for this sample, and T_m was not measured. The absorption spectrum was obtained by field-swept FID detection, followed by calculation of the power spectrum. Samples of OX063 (sodium salt) and trehalose in water were prepared gravimetrically with the OX063 concentration kept at 15mM. Samples containing trehalose were frozen by cooling the 4-mm outer-diameter quartz tube in liquid nitrogen before inserting it into the cooled cryostat. The sample without trehalose was placed in a 1.1-mm inner-diameter Teflon tube inside the 4-mm outer-diameter quartz tube to prevent breaking the tube and inserted into the cold cryostat in an He atmosphere without prefreezing. Air was not removed from the samples before freezing, as previous studies found no effect of air on spin lattice relaxation of trityls in frozen solution.

3 | RESULTS

To test the potential of trehalose as a biocompatible glassing agent, we recorded the polarization buildup curves of 4.7M ^{13}C urea, a potential marker for perfusion in patients with compromised renal function who cannot tolerate gadolinium or iodinated contrast agents,[17] in the presence of increasing amounts of trehalose. In the absence of trehalose, polarization of urea was slow and the buildup of polarization was negligible in clinically relevant timeframes[2] (Figure 1A, orange line). Imaging of a mouse leg xenograft with

hyperpolarized urea without trehalose yielded only noise with no discernable signal whatsoever (Figure 2A,C).

The addition of trehalose as a glassing agent markedly increased both the equilibrium polarization and buildup kinetics. Starting at 6.7%, the final signal increased rapidly with concentration before leveling off at approximately 15% trehalose (Figure 1B). A similar concentration dependence was also seen with the buildup rate (Figure 1C). In comparison with the standard glycerol preparation, trehalose solutions built up polarization much more quickly, but had a lower equilibrium polarization. The increase in polarization led to greatly enhanced imaging in vivo. Although the urea image without a glassing agent was completely noise, the addition of 20% trehalose in the polarization mixture resulted in a clear image with urea localized within the tumor (Figure 2B,D). To confirm that the results were not confined to urea, we repeated the polarization experiments with another difficult-to-polarize, non-self–glassing substrate, ^{13}C-labeled glycine, with similar results (Figure 1D).

Although trehalose is often cited as having unique molecular properties[19–23] that give it anomalous glass-forming and ice-breaking[24–26] capabilities, the molecular properties of trehalose have been the subject of considerable contention[27,28] other studies have suggested trehalose is not unique among carbohydrates in this regard.[29] To evaluate other potential carbohydrate glassing agents besides trehalose, we measured the polarization buildup of urea in the presence of equivalent amounts of analogous mono- and disaccharides (Figure 3). Trehalose was not unique in this context; fructose, glucose, and PEG400 all had slightly higher equilibrium polarization at an equivalent wt%. Sucrose had significantly lower equilibrium polarization, but similar buildup kinetics. In comparison, 20% trehalose was an effective compromise between fast buildup and equilibrium polarization, allowing efficient polarization within a clinically relevant timeframe.

The complex dependence of the polarization efficiency on the trehalose concentration in Figure 1 suggests a possible change in the microenvironment of the radical through a phase separation during freezing or other process. To gain a greater understanding of how trehalose may affect changes in the microenvironment of the OX063 radical during the DNP process, we recorded the EPR spectra and spin-lattice (T_1) and phase-memory dephasing (T_m) relaxation times of OX063 at 5K as a function of trehalose concentration (Figure 4). With roughly 10–60 times more trehalose than OX063 and the overall high concentrations of spins, it is likely that there are multiple environments for the radicals, some of which may be rather close neighbors of other radicals. Although the complexity of the system makes defining a quantitative physical model difficult, the differences in the microenvironment will likely be reflected in the T_1 relaxation times, as the most isolated of the radicals will have very long relaxation times based on the distance dependence of the dipolar interaction, and clusters of several radicals will have very short relaxation times from cross relaxation within the clusters.[30]

Changes in trehalose concentration resulted in dramatic changes in both the magnitude and distribution of relaxation times (Figure 4) of OX063. Without trehalose, the sample yielded an FID that could not be suppressed with attempts to decrease the magnetic field homogeneity and a short T_1 (~6–7 μs). This was also the narrowest spectrum, and discrete

structure was evident in the form of dipolar sidebands. A narrow linewidth and short T_1 relaxation time are both consistent with the water crystallizing upon freezing, causing high local concentrations of OX063 as the radical is preferentially excluded from the newly formed ice crystal. The echo-detected line shapes of the samples containing trehalose were considerably broader, likely reflecting a more inhomogeneous environment as the OX063 was no longer strictly confined to fast relaxing clusters, but was instead dispersed, albeit unevenly, throughout the sample. Inhomogeneity was evident in the relaxation as well—all of the trehalose samples exhibited wide ranges (orders of magnitude) in T_1 relaxation times. Multiple choices of time windows, therefore, had to be measured to include both the short relaxation times and the long relaxation times. Values of T_m were short, consistent with the high OX063 concentrations, and echo decays fit well with single exponentials.

At 5% trehalose, where DNP efficiency was similar to samples without trehalose (Figure 1), the T_1 relaxation was dominated by a fast relaxing population with a very short relaxation time (~ 0.8 μs)[30] (Figure 4B), similar to that found in the trehalose-free sample (data not shown). Two other minor populations, a distribution centered on 450 μs (10%) and another at 90 μs (~−2%), were also detected in addition to the fast relaxing species. Increasing concentrations of trehalose caused both a population shift towards the slower relaxing species (Figure 4C) and within the slower relaxing population, a shift towards slower relaxation times (Figure 4E). At 10% and 15% trehalose, where DNP efficiency was close to optimal (Figure 1), the long relaxing species was dominant (95% and 70%, respectively). The highest concentration, 30%, partially reversed this trend as there was a large shift in the distribution back to short relaxation times (55%). This concentration was near the eutectic point of trehalose/water mixtures,[18] and the reversal in trend for T_1 and linewidth may reflect the preferential freezing of water during the freezing process, although the exact interpretation is uncertain as the relative partitioning of OX063 between trehalose rich and poor phases is unknown. In contrast to the complex concentration dependence of the T_1 relaxation times, the linewidth decreased and T_m increased modestly and monotonically with the trehalose concentration (Figure 4F). Overall, as expected, there was a rough correspondence between the T_1 relaxation times and DNP buildup kinetics. In this case, longer relaxation times were associated with faster buildup kinetics, as expected for narrow linewidth radicals like OX063, where rapid spin diffusion exists and the solid effect is an important component in DNP transfer. Although not tested here, annealing may prove an efficient method for reducing inhomogeneities during the freezing process.[7,30–32]

4 | DISCUSSION

Solutions of trehalose have several potential advantages over the standard concentrated glycerol protocol. Although the equilibrium polarization is lower in the urea test case, the buildup rate is higher and the actual polarization is similar on the 15-−30-min time scales relevant for clinical use. Developments in coil design,[33] signal acquisition,[34] and postprocessing[35] have significantly increased the signal-to-noise ratio (SNR) since the inception of DNP MRI. The polarization process, however, is constrained by fundamental physics and will likely remain a choke point for clinical translation, especially if capital costs constrain work to a few research centers.[2] The ability to rapidly polarize a sample will likely be useful in this context.

Trehalose also has the advantage of being essentially biologically inert when injected intravenously. The extent to which glycerol's potential perturbation of metabolic activity is a concern will depend strongly on the pathway studied, but there is evidence that an acute challenge can alter a competing reaction even within the rapid time scale of the DNP experiment. Of particular concern is the rapid consumption of cytoplasmic ATP and FAD that an infusion of glycerol can cause by feeding the glycerol-3-phosphate shuttle. Marcos-Rius et al showed that a bolus of fructose several minutes before an injection of hyperpolarized ^{13}C DHAP caused a significant drop in labeled G3P and PEP resonances because of the depletion of the ATP and NAD pool.[36] Given that there are many metabolic reactions that are dependent on either ATP or are redox sensitive, this may be a concern as the pool of hyperpolarizable substrates continues to expand.

Several alternative methods have been proposed to improve polarization efficiency by preventing phase separation of the radical during the freezing. Lama et al modified the rate of freezing by freezing the samples in liquid-nitrogen–cooled isopentane, rather than directly in liquid nitrogen, as is typically used.[37,38] The result is a homogenous frozen solid that polarizes rapidly and efficiently, regardless of the glassing properties of the original solution. The disadvantage for clinical applications is the possibility of residual traces of isopentane in the product, which are not removed by the filtering process and cannot be assayed easily. Phase separation can also be prevented by impregnating the radical in a solid matrix hybrid polarizing solids (HYPSOs and related methods),[39,40] but the final polarization is currently less than a purely liquid formulation. Optimization of polarizing conditions and pulse sequences[41] will likely play a key role in the expansion of DNP MRI in the future.[7,42]

Funding information

NCI; National Institutes of Health, Grant/Award Number: R01CA177744

REFERENCES

1. Keshari KR, Wilson DM. Chemistry and biochemistry of C-13 hyperpolarized magnetic resonance using dynamic nuclear polarization. Chem Soc Rev. 2014;43:1627–1659. [PubMed: 24363044]
2. Kurhanewicz J, Vigneron DB, Ardenkjaer-Larsen JH, et al. Hyperpolarized (13)C MRI: path to clinical translation in oncology. Neoplasia. 2019;21:1–16. [PubMed: 30472500]
3. Gray LR, Tompkins SC, Taylor EB. Regulation of pyruvate metabolism and human disease. Cell Mol Life Sci. 2014;71:2577–2604. [PubMed: 24363178]
4. Tan KO, Mardini M, Yang C, Ardenkjaer-Larsen JH, Griffin RG. Three-spin solid effect and the spin diffusion barrier in amorphous solids. Sci Adv. 2019;5;eaax2743. 10.1126/sciadv.aax2743. [PubMed: 31360772]
5. Thankamony ASL, Wittmann JJ, Kaushik M, Corzilius B. Dynamic nuclear polarization for sensitivity enhancement in modern solid-state NMR. Prog Nucl Mag Res Sp. 2017;102:120–195.
6. Ludwig C, Marin-Montesinos I, Saunders MG, Gunther UL. Optimizing the polarization matrix for ex situ dynamic nuclear polarization. J Am Chem Soc. 2010;132:2508–2509. [PubMed: 20131776]
7. Leavesley A, Wilson CB, Sherwin M, Han S. Effect of water/glycerol polymorphism on dynamic nuclear polarization. Phys Chem Chem Phys. 2018;20:9897–9903. [PubMed: 29619477]
8. Frank MSB, Hilty MD, Nahata MC. Glycerol: a review of its pharmacology, pharmacokinetics, adverse reactions, and clinical use. Pharmacotherapy. 1981;1:147–160. [PubMed: 6927604]
9. Tao RC, Kelley RE, Yoshimura NN, Benjamin F. Glycerol: its metabolism and use as an intravenous energy-source. Jpen-Parenter Enter. 1983;7:479–488.

10. Hibuse T, Maeda N, Nagasawa A, Funahashi T. Aquaporins and glycerol metabolism. BBA-Biomembranes. 2006;1758:1004–1011. [PubMed: 16487477]
11. Richards AB, Krakowka S, Dexter LB, et al. Trehalose: a review of properties, history of use and human tolerance, and results of multiple safety studies. Food Chem Toxicol. 2002;40:871–898. [PubMed: 12065209]
12. Ni CH, Gong YY, Liu XJ, Sun CQ, Zhou ZF. The anti-frozen attribute of sugar solutions. J Mol Liquids. 2017;247:337–344.
13. Vanelburg RM, Uil JJ, Kokke FTM, et al. Repeatability of the sugar absorption test, using lactulose and mannitol, for measuring intestinal permeability for sugars. J Pediatr Gastr Nutr. 1995;20:184–188.
14. Eaton SS, Eaton GR. Relaxation times of organic radicals and transition metal ions. In: Berliner LJ, Eaton GR, Eaton SS, eds. Distance Measurements in Biological Systems by EPR. Boston, MA: Springer, US; 2000:29–154.
15. Borgia GC, Brown RJS, Fantazzini P. Uniform-penalty inversion of multiexponential decay data - II. Data spacing, T-2 data, systematic data errors, and diagnostics. J Magn Reson. 2000;147:273–285. [PubMed: 11097819]
16. Borgia GC, Brown RJS, Fantazzini P. Uniform-penalty inversion of multiexponential decay data. J Magn Reson. 1998;132:65–77. [PubMed: 9615412]
17. von Morze C, Larson PE, Hu S, et al. Imaging of blood flow using hyperpolarized [(13)C]urea in preclinical cancer models. J Magn Reson Imaging. 2011;33:692–697. [PubMed: 21563254]
18. Roe KD, Labuza TP. Glass transition and crystallization of amorphous trehalose-sucrose mixtures. Int J Food Prop. 2005;8:559–574.
19. Engelsen SB, Perez S. Unique similarity of the asymmetric trehalose solid-state hydration and the diluted aqueous-solution hydration. J Phys Chem B. 2000;104:9301–9311.
20. Magazu S, Maisano G, Migliardo P, Tettamanti E, Villari V. Transport phenomena and anomalous glass-forming behaviour in alpha, alpha-trehalose aqueous solutions. Mol Phys. 1999;96:381–387.
21. Branca C, Magazu S, Maisano G, Migliardo P. Anomalous cryoprotective effectiveness of trehalose: Raman scattering evidences. J Chem Phys. 1999;111:281–287.
22. Shiraga K, Adachi A, Nakamura M, Tajima T, Ajito K, Ogawa Y. Characterization of the hydrogen-bond network of water around sucrose and trehalose: microwave and terahertz spectroscopic study. J Chem Phys. 2017;146:105102. [PubMed: 28298096]
23. Lerbret A, Bordat P, Affouard F, et al. Influence of homologous disaccharides on the hydrogen-bond network of water: complementary Raman scattering experiments and molecular dynamics simulations. Carbohyd Res. 2005;340:881–887.
24. Whelan AP, Regand A, Vega C, Kerry JP, Goff HD. Effect of trehalose on the glass transition and ice crystal growth in ice cream. Int J Food Sci Tech. 2008;43:510–516.
25. Wang GM, Haymet ADJ. Trehalose and other sugar solutions at low temperature: modulated differential scanning calorimetry (MDSC). J Phys Chem B. 1998;102:5341–5347.
26. Crowe LM, Reid DS, Crowe JH. Is trehalose special for preserving dry biomaterials? Biophys J. 1996;71:2087–2093. [PubMed: 8889183]
27. Shiraga K, Suzuki T, Kondo N, De Baerdemaeker J, Ogawa Y. Quantitative characterization of hydration state and destructuring effect of monosaccharides and disaccharides on water hydrogen bond network. Carbohyd Res. 2015;406:46–54.
28. Lee SL, Debenedetti PG, Errington JR. A computational study of hydration, solution structure, and dynamics in dilute carbohydrate solutions. J Chem Phys. 2005;122:204511. [PubMed: 15945756]
29. Levine H Another view of trehalose for drying and stabilizing biological materials. Bio Pharm. 1992;5:36–40.
30. Chen HJ, Maryasov AG, Rogozhnikova OY, Trukhin DV, Tormyshev VM, Bowman MK. Electron spin dynamics and spin-lattice relaxation of trityl radicals in frozen solutions. Phys Chem Chem Phys. 2016;18:24954–24965. [PubMed: 27560644]
31. Marin-Montesinos I, Paniagua JC, Vilaseca M, et al. Self-assembled trityl radical capsules-implications for dynamic nuclear polarization. Phys Chem Chem Phys. 2015;17:5785–5794. [PubMed: 25626422]

32. Marin-Montesinos I, Paniagua JC, Peman A, et al. Paramagnetic spherical nanoparticles by the self-assembly of persistent trityl radicals. Phys Chem Chem Phys. 2016;18:3151–3158. [PubMed: 26742686]
33. Sanchez-Heredia JD, Szocska Hansen ES, Laustsen C, Zhurbenko V, Ardenkjaer-Larsen JH. Low-noise active decoupling circuit and its application to (13)C cryogenic RF coils at 3T. Tomography. 2017;3:60–66. [PubMed: 30042972]
34. Xing Y, Reed GD, Pauly JM, Kerr AB, Larson PE. Optimal variable flip angle schemes for dynamic acquisition of exchanging hyperpolarized substrates. J Magn Reson. 2013;234:75–81. [PubMed: 23845910]
35. Brender JR, Kishimoto S, Merkle H, et al. Dynamic imaging of glucose and lactate metabolism by 13C-MRS without hyperpolarization. Sci Rep. 2019;9:3410. [PubMed: 30833588]
36. Marco-Rius I, von Morze C, Sriram R, et al. Monitoring acute metabolic changes in the liver and kidneys induced by fructose and glucose using hyperpolarized [2-C-13]dihydroxyacetone. Magn Reson Med. 2017;77:65–73. [PubMed: 27859575]
37. Lama B, Collins JHP, Downes D, Smith AN, Long JR. Expeditious dissolution dynamic nuclear polarization without glassing agents. NMR Biomed. 2016;29:226–231. [PubMed: 26915792]
38. Bray RC. Sudden freezing as a technique for the study of rapid reactions. Biochem J. 1961;81:189–193. [PubMed: 13872669]
39. Gajan D, Schwarzwalder M, Conley MP, et al. Solid-phase polarization matrixes for dynamic nuclear polarization from homogeneously distributed radicals in mesostructured hybrid silica materials. J Am Chem Soc. 2013;135:15459–15466. [PubMed: 23978152]
40. Gajan D, Bornet A, Vuichoud B, et al. Hybrid polarizing solids for pure hyperpolarized liquids through dissolution dynamic nuclear polarization. Proc Natl Acad Sci USA. 2014;111:14693–14697. [PubMed: 25267650]
41. Bornet A, Melzi R, Perez Linde AJ, et al. Boosting dissolution dynamic nuclear polarization by cross polarization. J Phys Chem Lett. 2013;4:111–114. [PubMed: 26291221]
42. Capozzi A, Patel S, Wenckebach WT, Karlsson M, Lerche MH, Ardenkjaer-Larsen JH. Gadolinium effect at high-magnetic-field DNP: 70% (13)C polarization of [U-(13)C] glucose using trityl. J Phys Chem Lett. 2019;10:3420–3425. [PubMed: 31181932]

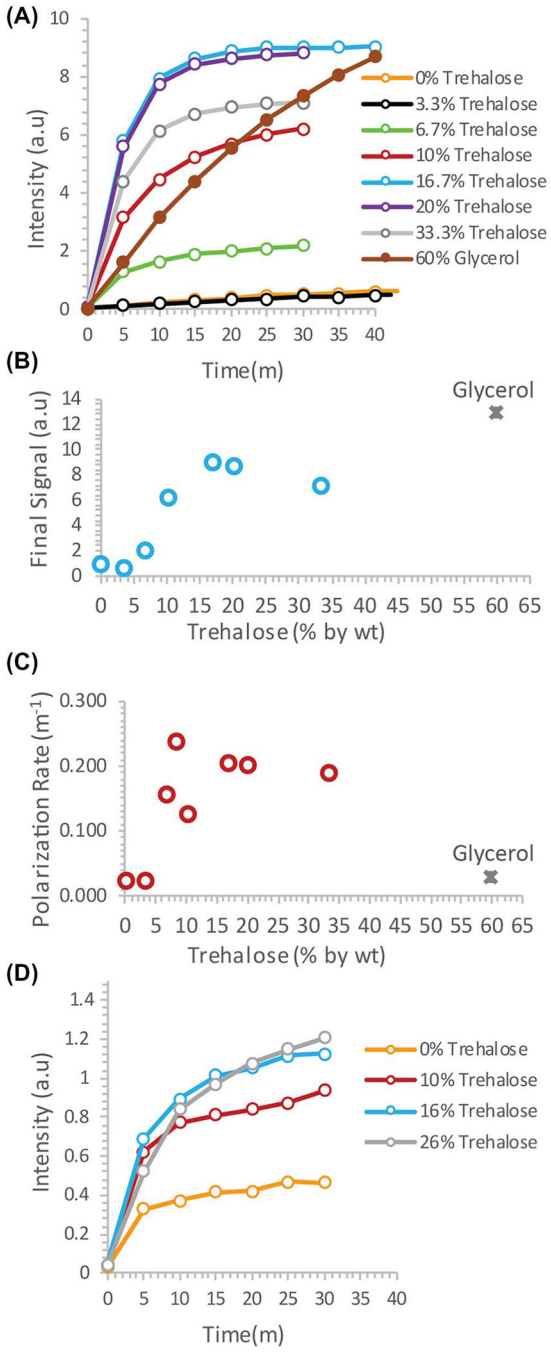

FIGURE 1.

A, Dynamic nuclear polarization (DNP) buildup of 4.7M ^{13}C urea in trehalose solutions versus the current 60% glycerol protocol. B and C, Plot of the final signal (B) and polarization rate (C) as a function of the trehalose concentration. D, DNP buildup of 3M ^{13}C glycine with increasing concentrations of trehalose as a glassing agent

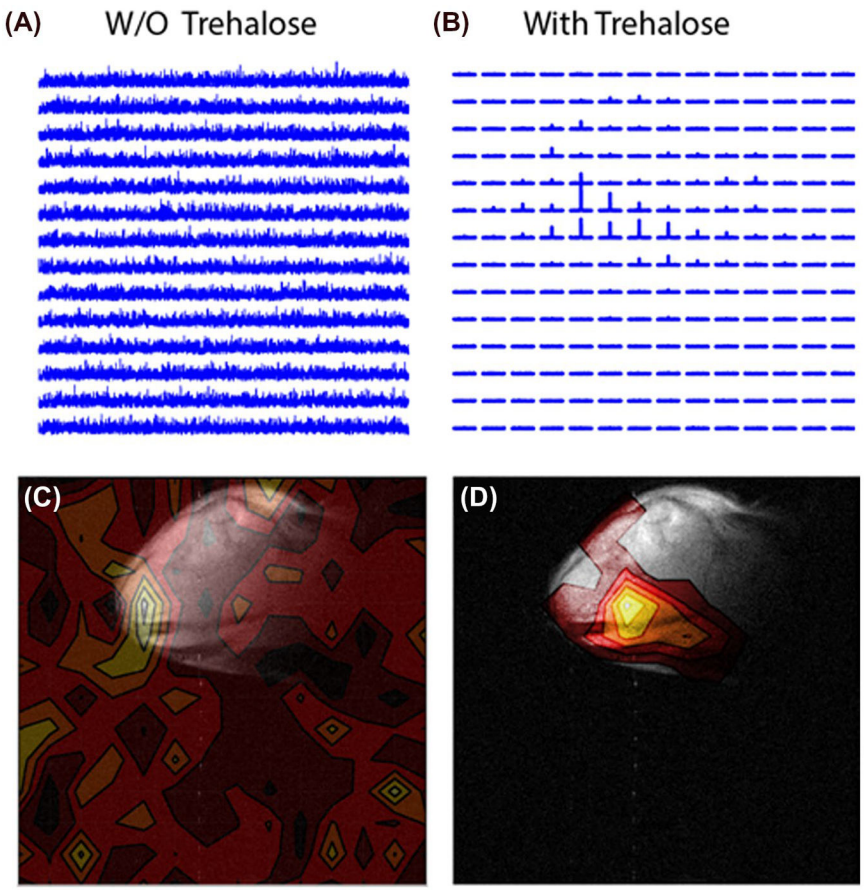

FIGURE 2.

A and C, Imaging of a mouse leg xenograft by chemical shift imaging with hyperpolarized ^{13}C urea in the absence of a glassing agent. B and D, The same mouse leg imaged using 15% trehalose as a glassing agent. A clear signal is evident within the tumor only when trehalose is used as a glassing agent

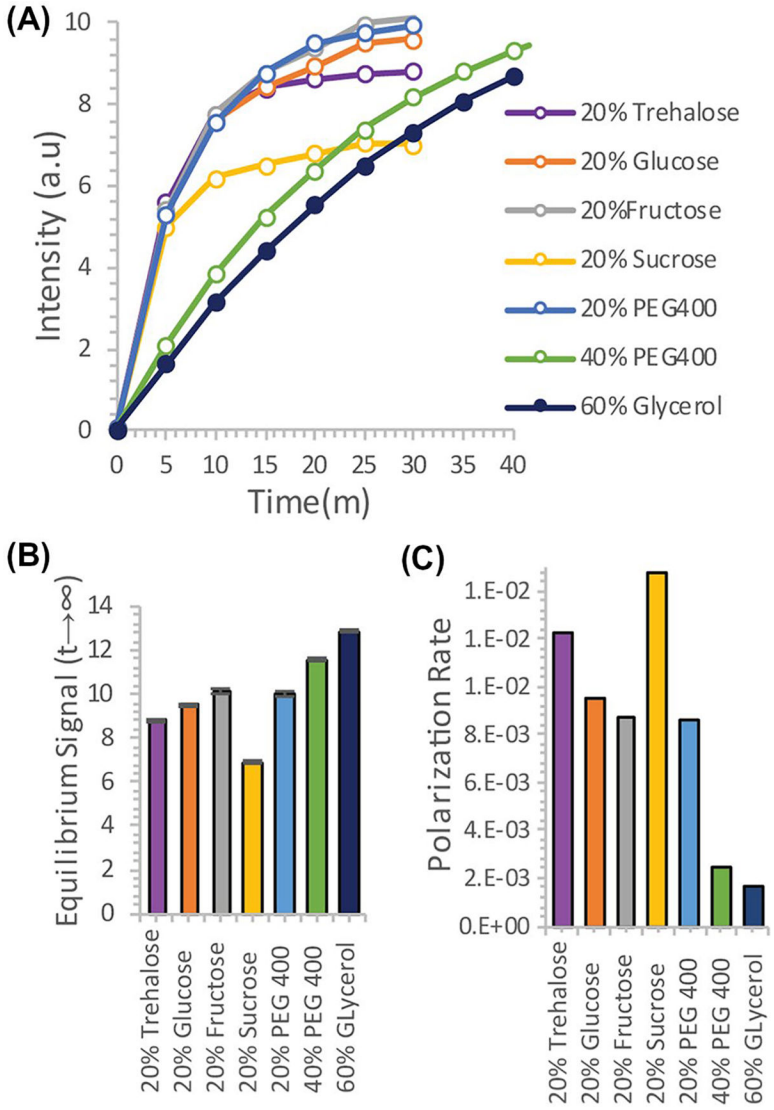

FIGURE 3.

A, Dynamic nuclear polarization (DNP) buildup of 4.7M ^{13}C urea using trehalose solutions as a glassing agent versus equivalent polyalcohols. B and C, Plot of the final signal (B) and polarization rate (C) for the different polyalcohols

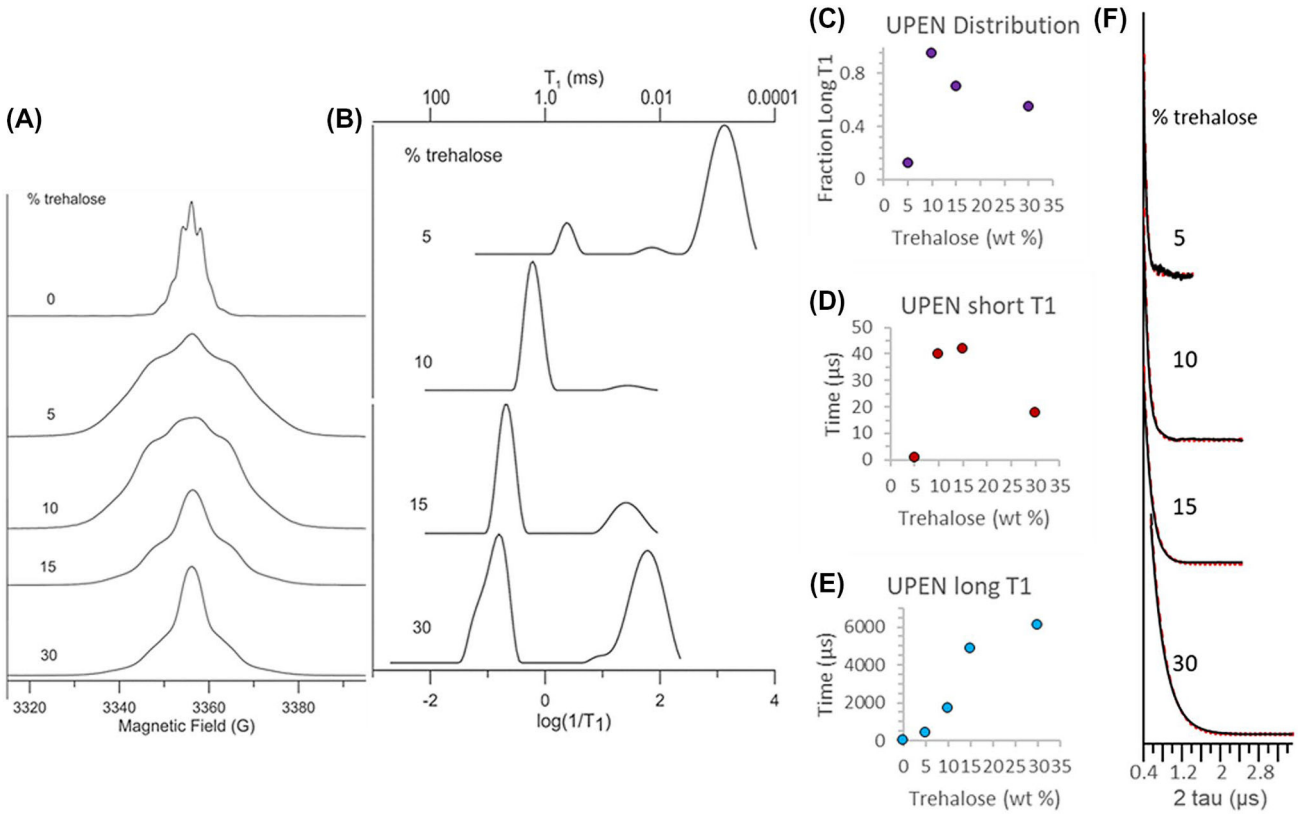

FIGURE 4.

A, EPR absorption spectra at 5 K for 15mM OX063 in aqueous samples containing 0%, 5%, 10%, 15%, or 30% by weight trehalose. B, Probability distributions of T_1 (ms) for 15mM solutions of OX063 in water:trehalose mixtures calculated using UPEN from inversion recovery curves at 5 K. C, Fraction of long T_1 times as a function of the trehalose concentration from UPEN analysis. D and E, Mean T_1 relaxation times for the short (D) and long (E) fractions. F, Two pulse echo decays as a function of trehalose concentration. Black is the experimental data, red is the fit with single exponentials